International Journal of Solids and Structures 46 (2009) 1305–1316

Contents lists available at ScienceDirect

International Journal of Solids and Structures

journal homepage: www.elsevier.com/locate/ijsolstr

Deformation behaviour of paper and board subjected to moisture diffusion

Marie-Laure Dano *, Jean-Pierre Bourque

Department of Mechanical Engineering, Université Laval, Pavillon Adrien-Pouliot, Québec, Canada G1V0A6

ARTICLE INFO

Article history:
Received 9 July 2008
Received in revised form 26 September 2008
Available online 12 November 2008

Keywords:
Paper
Cardboard
Laminate
Hygro-mechanical
Ritz method
Transient
Warping
Nonlinear plate theory
Finite element
Instability

ABSTRACT

This paper presents a method to predict the through-thickness moisture content distribution and associated induced deformations of paper and cardboard sheets as they are subjected to relative humidity changes. The transient moisture diffusion problem is solved using a "natural" analytic approach that has previously been applied for solving transient heat conduction in multi-layer solids. The deformation behaviour of the sheet during the moisture diffusion process is predicted using a semi-analytical approach based on a Rayleigh–Ritz minimization of the total potential energy. Geometrically nonlinear effects are taken into account. Curvatures of the originally flat sheet are predicted as a function of time, as are the shapes of the sheet for steady-state condition. As multiple solutions exist, stability is studied. The developed model was used to study the deformation behaviour of one paper and two cardboard sheets. Comparisons with finite-element results demonstrate that the developed model provides accurate results. The displacements obtained for steady-state conditions are within +6%. Comparisons with previous steady-state analyses reveal important differences in the shape of one cardboard sheet. This suggests that the moisture diffusion process may influence the configuration assumed by the sheet at steady-state equilibrium. Hence, it may be necessary to take the moisture diffusion into account in the analysis to accurately predict the hygro-mechanical behaviour of paper or cardboard sheets.

1. Introduction and background

During the last decade, dimensional instability and curl of paper and cardboard have become an important issue for the pulp and paper, and the printing industries. Curl can be defined as the out-of-plane deformation of an initially flat sheet and is induced by changes in the ambient humidity or temperature. Any paper or cardboard with an unsymmetric layered construction will curl and become cylindrical when subjected to humidity changes. In addition, non-uniform drying conditions will lead to curl. Since the curl problem has significant economic impact on the paper industry, several studies have been conducted to better understand the problem and propose strategies to increase the dimensional stability of paper sheets. In this paper a study conducted to predict the transient moisture-induced mechanical behaviour of paper and cardboard sheets is presented.

The moisture-induced mechanical behaviour of paper has been the subject of several studies. Carlsson (1981) used classical lamination theory based on linear kinematics to predict curl of papers. The analysis predicted that the paper sheet would assume a double-curvature shape whereas experimental observations indicate a single curvature. The reason for the difference can be explained by the large displacement magnitude which invalidates the use of linear kinematics. Hyer (1981a) observed a similar phenomenon when he studied the cured shapes of unsymmetric carbon/epoxy laminates. Later, Hyer (1981b) proposed a geometrically non linear model based on a Rayleigh–Ritz minimization of the total potential energy to predict the cured shape of cross-ply unsymmetric laminates. Nordstrom et al. (1998) used Hyer's model to study the deformation behaviour of paper sheets subjected to humidity change. They also performed geometrically non linear finite-element analyses which correlated well with Hyer's model. A few studies have examined the viscoelastic influence on paper curl. In particular, Lu and Carlsson (2001) investigated the effect of viscoelastic stress relaxation on the curl response of paper subjected to transient humidity change. The predicted curvature response versus time was in reasonable agreement with experimental measurements although their predictions underestimated the curvature change during the moisture content increase. The authors concluded that a model which takes the moisture diffusion process through the thickness of the sheet into account would lead to more accurate predictions. However, this has not yet been achieved.

Similar work has also been detailed in the literature on cardboard curl. Gendron et al. (2004) studied the hygro-mechanical behaviour of two cardboard layups. They used a model based on the approach proposed by Hyer (1981b) and a steady-state geometrically non linear finite-element model. The results showed that both models provide very similar results and that different equilibrium shapes can be obtained depending on the type of

* Corresponding author.
E-mail address: mldano@gmc.ulaval.ca (M.-L. Dano).

0020-7683/$ - see front matter © 2008 Elsevier Ltd. All rights reserved.
doi:10.1016/j.ijsolstr.2008.10.035

Nomenclature

a, b, c, d	coefficients
D_i	effective diffusion of the ith layer
f_a, f_b, f_c, f_d	equilibrium equations
H	thickness of the N-layer sheet
h_0, h_N	convective mass transfer coefficients at the outer boundary surfaces
J	number of intervals
k_i	effective diffusivity of the ith layer
L_x, L_y	length of the sheet in the x-and y-directions
M_i	moisture content for the ith layer
$M_{lin,i,j}$	linear moisture distribution function for the jth interval of the the ith layer
M_{lin}	piecewise-linear moisture distribution function for the N-layer sheet
M_0	uniform initial moisture content of the N-layer sheet
M_∞	equilibrium moisture content of the N-layer sheet at RH_∞
N_m	normalization integral (norm)
N	number of layers
p	number of eigenvalues
$\overline{Q}_{ij}$	transformed reduced stiffness coefficients of an individual layer
RH_0	initial ambient relative humidity
RH_∞	ambient relative humidity
s_m	integration coefficients
t	time
t_p	particular given time
u^0, v^0, w^0	midplane displacements in the x-, y-, and z-directions
x, y, z	space coordinates
z_0, z_N	value of the space coordinate at the outer boundary surfaces
z_i	value of the space coordinate at the inner boundary surfaces ($i = 1,\ldots, N\text{-}1$)
$\widetilde{Z}_{i,m}$	mth eigenfunction
ΔM	change in moisture content
ε_x, ε_y	total strains in the x-and y-directions
$\varepsilon_x^0, \varepsilon_y^0$	total midplane strains in the x-and y-directions
$\phi_{i,m}$	functions defined in de Monte (2002)
γ_{xy}	total engineering shear strain in the x-y plane
γ_{xy}^0	total midplane engineering shear strain in the x-y plane
$\kappa_x,\kappa_y,\kappa_{xy}$	midplane curvatures
λ_m	mth eigenvalue
Π	total potential energy of the N-layer sheet
θ_i	difference in moisture content for the ith layer: $M_\infty - M_i$
θ_0	difference in moisture content for the ith layer: $M_\infty - M_0$
ρ_i	density of the ith layer

cardboard, moisture content change, and sheet dimension. Finally, models have been proposed to predict moisture diffusion in cellulosic materials such as paper and wood. Traditionally, moisture diffusion has been modelled using Fick's second law (Skaar, 1958; Chen et al., 1995; Baronas and Ivanauska, 2004) which assumes that material is homogeneous and has a constant diffusivity. However, the diffusion process through paper is more complex since moisture is transported within the fibers, along the fiber surfaces or through the pores (Hägglund et al., 1999). To take these effects into account, multiphase models have been proposed (Hägglund et al., 1999; Bandyopadhyay et al., 2002). These models present the drawback of using variables, such as pore diffusivity, which are impossible to experimentally determine directly and an inverse method has to be used for variable identification.

This study focuses on predicting the transient response of paper or cardboard sheets subjected to through-thickness moisture diffusion. The objective is to study the development of curl during the moisture diffusion process. To achieve this objective, the through-thickness moisture content distribution is predicted as a function of time and, for each time increment, the moisture-induced deformation is computed. As multiple equilibrium configurations were expected, a semi-analytical approach, such as the one proposed by Hyer (1981b), was used as it would be more convenient and would give more insight into the curl response than using a finite-element model. However, the finite-element software ABAQUS is used to validate the predictions of the semi-analytical model.

The rest of the paper is organised as follows. First, a model is developed to predict the moisture content distribution through thickness as a function of time. This model is based on de Monte's (2002) work that proposed a "natural" analytic approach for solving one dimensional transient heat conduction in multi-layer composites. Next, the predicted moisture content distribution is applied to the sheet and the induced-deformation is calculated. A model using Hyer's (1981b) approach is then developed to perform the calculations. The model that takes geometrically non linearities and the through-thickness moisture content distribution into account is based on a Rayleigh–Ritz minimization of the total potential energy. By solving these equations, the deformations induced by moisture diffusion in the paper or cardboard sheet are predicted as a function of time. After the theory is presented, numerical results for different paper and cardboard sheets are discussed. Finally the model predictions are compared with finite-element results obtained with ABAQUS.

2. Model development

2.1. Moisture content distribution prediction

2.1.1. Transient moisture diffusion equations and analytical solution

The model is developed for a paper or a cardboard sheet made of N-layers as shown in Fig. 1. The figure illustrates a cross-sectional view in the x–z plane. The origin of the through-thickness coordinate, noted z, is located at the geometric midplane of the sheet. The z-coordinates indicated in the figure are the locations of the top and bottom surfaces of each ply. Each layer is assumed to have a constant density r_i and an effective diffusion coefficient D_i ($i = 1,\ldots,N$). The sheet is initially ($t = 0$) in equilibrium with air at a relative humidity RH_0. The sheet has a uniform moisture content M_0. Suddenly, at $t = 0$, the ambient relative humidity changes to RH_∞ and the sheet is subjected to moisture flux through both boundary surfaces, at $z = z_0$ and $z = z_N$. After the sheet reaches equilibrium, the moisture content is equal to M_∞. Since the sheet thickness is small relative to its length and width, it is reasonable to assume that moisture movement occurs exclusively in the z-direction. The moisture transport process is treated as a diffusion problem based on Fick's second law. The diffusion model may not be as accurate as a multiphase model but is much simpler to implement. The transient moisture movement based on Fick's second law can be expressed using the diffusion equation formulated in a one dimensional space by

$$\frac{\partial^2 \theta_i}{\partial z^2} = \frac{1}{D_i}\frac{\partial \theta_i}{\partial t}, \quad z \in [z_{i-1}, z_i], \quad i = 1,\ldots,N, \tag{1}$$

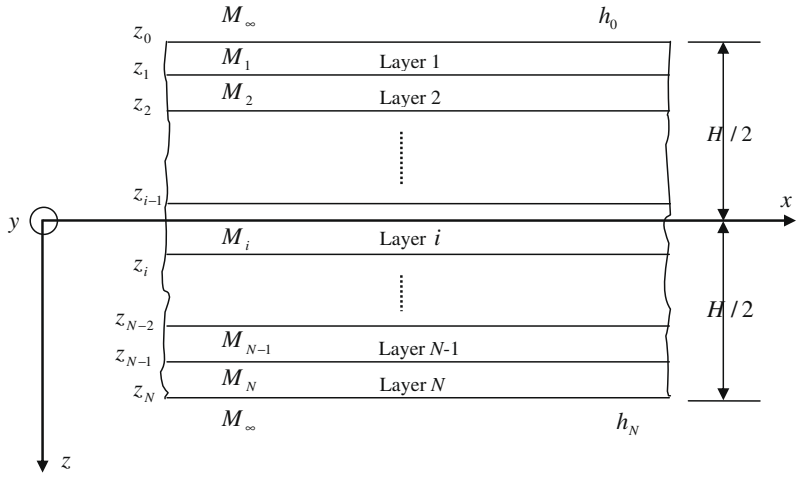

Fig. 1. Representation of a multi-layer paper or cardboard sheet.

where $\theta_i = \theta_i(z,t) = M_\infty - M_i(z,t)$ is the difference in moisture content between the equilibrium moisture content at RH_∞ and the moisture content in the ith-layer, at position z and time t. The initial condition (at $t = 0$) specifies that the initial moisture content is uniform and equal to M_0. It can be expressed as

$$\theta_i(z, t=0) = \theta_0, \quad z \in [z_{i-1}, z_i], \quad i = 1, \ldots, N, \tag{2}$$

where $\theta_0 = M_\infty - M_0$ is the difference in moisture content between the equilibrium moisture content at RH_∞ and the initial moisture content. For $t > 0$, both boundary surfaces of the sheet are subjected to convective moisture flux. These outer boundary conditions can be written as,

$$-k_1\left(\frac{\partial\theta_1}{\partial z}\right)_{z_0} + h_0\theta_1(z_0,t) = 0, \tag{3}$$

$$k_N\left(\frac{\partial\theta_N}{\partial z}\right)_{z_N} + h_N\theta_N(z_N,t) = 0, \tag{4}$$

where $k_1 = D_1\rho_1/100$ and $k_N = D_N\rho_N/100$ are the effective diffusivity coefficients of the first and Nth-layers, respectively. Quantities h_0 and h_N are the convective mass transfer coefficients for the outer surface at $z = z_0$ and the outer surface at $z = z_N$, respectively. They are assumed to be uniform and constant. The contact between adjacent layers is assumed to be perfect. Therefore, the moisture content and the moisture flux are continuous at the surface of two adjacent layers. These continuity conditions can be expressed as,

$$\theta_i(z_i,t) = \theta_{i+1}(z_i,t), \quad i = 1, \ldots, N-1, \tag{5}$$

$$k_i\left(\frac{\partial\theta_i}{\partial z}\right)_{z_i} = k_{i+1}\left(\frac{\partial\theta_{i+1}}{\partial z}\right)_{z_i}, \quad i = 1, \ldots, N-1, \tag{6}$$

where $k_i = D_i\rho_i/100$ is the effective diffusivity coefficient of ith-layer.

The set of Eqs. (1)–(6) can be solved using the "natural" analytic technique proposed by de Monte (2002) for solving transient heat conduction in a multi-layer composite laminate. The set of equations obtained by de Monte has exactly the same form as Eqs. (1)–(6), in which moisture content, moisture diffusion, and moisture diffusivity are replaced by temperature, thermal diffusivity and thermal conductivity, respectively. The solution of the equations set is obtained using the method of separation of variables. When separating the variables, the effective moisture diffusion coefficient D_i of each layer is retained on the side of the modified moisture diffusion equation where the time-dependent functions are collected. It results in a transcendental equation for the determination of the eigenvalues that are simpler than the ones obtained when using traditional techniques. A new type of orthogonality relationship was developed and used to obtain the final complete series solution. It was felt that numerous derivations of the equations that lead to the solution were not necessary as they are all indicated in de Monte (2002). Using this approach, the solution of the set of equations can be written as,

$$\theta_i(z,t) = \sum_{m=1}^{\infty} s_m\phi_{i,m}\widetilde{Z}_{i,m}(z)\mathrm{e}^{-\lambda_m^2 D_1 t}, \quad z \in [z_{i-1}, z_i], \quad i = 1, \ldots, N, \tag{7}$$

where s_m is given by,

$$s_m = \frac{\theta_0}{N_m}\sum_{i=1}^{N}\phi_{i,m}\left(\frac{k_i}{D_i}\right)\left\{-\left[\frac{\widetilde{Z}'_{i,m}(z)}{\lambda_m^2(D_1/D_i)}\right]_{z_{i-1}}^{z_i}\right\}, \quad i = 1, \ldots, N. \tag{8}$$

In Eqs. (7) and (8), $\phi_{i,m}$ are functions defined in de Monte (2002), λ_m is the mth eigenvalue, $\widetilde{Z}_{i,m}(z)$ is the mth eigenfunction corresponding to the mth eigenvalue λ_m in the ith layer and N_m is the normalization integral (norm) associated with the mth eigenvalue λ_m. Substituting the definitions of the moisture content difference $\theta_i(z,t) = M_\infty - M_i(z,t)$ and $\theta_0 = M_\infty - M_0$ into Eqs. (7) and (8) and rearranging the terms lead to

$$M_i(z,t) = M_\infty - (M_\infty - M_0)\sum_{m=1}^{\infty}\frac{1}{N_m}\left\{\sum_{i=1}^{N}\phi_{i,m}\left(\frac{k_i}{D_i}\right)\left[\frac{\widetilde{Z}'_{i,m}(z)}{\lambda_m^2(D_1/D_i)}\right]_{z_{i-1}}^{z_i}\right\}$$
$$\phi_{i,m}\widetilde{Z}_{i,m}(z)\mathrm{e}^{-\lambda_m^2 D_1 t}, \quad z \in [z_{i-1}, z_i], \quad i = 1, \ldots, N \tag{9}$$

which gives the distribution of the moisture content through the thickness of the N-layer sheet.

The software *MATHEMATICA*® (Wolfram, 1996) was used to compute and solve the set of equations using de Monte's, (2002) technique. The developed model allows determining the distribution of the moisture content in a paper or cardboard sheet made of N layers as a function of time. The number p of eigenvalues used in the series solution, Eq. (9), was set to 30. This number was selected because it offered a good compromise between accuracy of the approximate solution and reasonable computation time.

2.1.2. Piecewise linearization of the moisture content distribution solution

The obtained solution gives the moisture content as a function of time and the z-coordinate for each layer. Since the expression is quite complex, it will require lengthy computation if it is directly used to compute moisture induced-deformations. Therefore, the

solution obtained for each layer was approximated for given times t_p by a piecewise-linear function.

Each layer was partitioned into J-intervals. The coordinates $(z_{i,j-1}, z_{i,j})$ of the jth interval of the ith layer are given by

$$z_{i,j} = z_{i-1} + j\frac{(z_i - z_{i-1})}{J}, \quad i = 1,\ldots,N, \quad j = 1,\ldots,J, \tag{10}$$

where z_i represents the location of each layer. For a particular time $t = t_p$, the moisture content distribution obtained for the ith layer is approximated for each interval by a linear function. The resulting piecewise-linear function can be written for the ith layer as

$$M_{lin,i,j}(z) = M(z_{i,j-1}, t_p) + \left(\frac{M(z_{i,j}, t_p) - M(z_{i,j-1}, t_p)}{z_{i,j} - z_{i,j-1}}\right)z, \quad j = 1,\ldots,J. \tag{11}$$

Hence, the moisture content distribution for a N-layer sheet at $t = t_p$ can be expressed as:

$$M_{lin}(z) = M_{lin,i,j}(z), \quad z_{i,j-1} \leqslant z \leqslant z_{i,j}, \quad i = 1,\ldots,N, \quad j = 1,\ldots,J. \tag{12}$$

2.2. Moisture-induced deformation prediction

Once the moisture content distribution can be predicted for a particular time $t = t_p$, the associated moisture-induced deformation may be calculated. The model developed to predict the response of a multi-layer paper or cardboard sheet to a through-thickness moisture content distribution is based on Hyer's (1981b) approach. It is an extension of classical lamination theory which accounts for geometrical nonlinearities. Polynomial approximations of displacements are used in the expression of the total potential energy and the Rayleigh–Ritz technique is applied.

Table 1
Properties of the three-layer paper sheet.

	Layer 1	Layer 2	Layer 3
Thickness (mm)			
h	0.100	0.132	0.115
Density (kg/m^3)			
ρ	448	343	535
Young's moduli (GPa)			
E_x	4.41	3.09	4.04
E_y	2.01	1.02	4.04
Shear modulus (GPa)			
G_{xy}	1.04	0.59	1.46
Poisson's ratio			
ν_{yx}	0.12	0.12	0.27
Moisture expansion coefficient (10^{-3}/%)			
β_x	0.46	0.38	0.56
Moisture expansion coefficient (10^{-3}/%)			
β_y	1.38	1.57	0.56
Effective diffusion coefficient (10^{-11} m^2/s)			
D	6.90	13.92	7.73

2.2.1. Computation of the total potential energy

Assuming a state of plane-stress, the total potential energy of the multi-layer sheet, Π, can be expressed as a function of material and geometric properties of the sheet, moisture content change ΔM, and the total strains by

$$\begin{aligned}\Pi = \frac{1}{2}\int_{-L_x/2}^{L_x/2}\int_{-L_y/2}^{L_y/2}\int_{-H/2}^{H/2}\Big(&\frac{1}{2}\overline{Q}_{11}\varepsilon_x^2 + \overline{Q}_{12}\varepsilon_y\varepsilon_x + \overline{Q}_{16}\gamma_{xy}\varepsilon_x \\ &+ \frac{1}{2}\overline{Q}_{22}\varepsilon_y^2 + \overline{Q}_{26}\gamma_{xy}\varepsilon_y + \frac{1}{2}\overline{Q}_{66}\gamma_{xy}^2 \\ &- \Big(\overline{Q}_{11}\alpha_x + \overline{Q}_{12}\alpha_y + \overline{Q}_{16}\alpha_{xy}\Big)\varepsilon_x\Delta M \\ &- \Big(\overline{Q}_{12}\alpha_x + \overline{Q}_{22}\alpha_y + \overline{Q}_{26}\alpha_{xy}\Big)\varepsilon_y\Delta M \\ &-(\overline{Q}_{16}\alpha_x + \overline{Q}_{26}\alpha_y + \overline{Q}_{66}\alpha_{xy})\gamma_{xy}\Delta M\Big)\,dx\,dy\,dz,\end{aligned} \tag{13}$$

where L_x, L_y, and H are the lengths of the sheet in the x- and y-directions, and its thickness. The $\overline{Q}_{ij}$ terms are the transformed reduced stiffness of the individual layer. Using the piecewise-linear function defined by Eq. (12), the change in moisture content ΔM can be expressed at a particular time $t = t_p$ as

$$\Delta M(z) = M_{lin}(z) - M_0. \tag{14}$$

This equation applies the moisture content distribution determined by the moisture diffusion model at time $t = t_p$ so that the deformation induced by the moisture content change can be calculated.

The total strains ε_x, ε_y, γ_{xy} are given by

$$\begin{Bmatrix}\varepsilon_x\\ \varepsilon_y\\ \gamma_{xy}\end{Bmatrix} = \begin{Bmatrix}\varepsilon_x^0\\ \varepsilon_y^0\\ \gamma_{xy}^0\end{Bmatrix} + z\begin{Bmatrix}\kappa_x\\ \kappa_y\\ \kappa_{xy}\end{Bmatrix}. \tag{15}$$

The quantities $\varepsilon_x^0, \varepsilon_y^0, \gamma_{xy}^0$ and κ_x, κ_y, κ_{xy} are the total midplane strains and curvatures, respectively, defined by

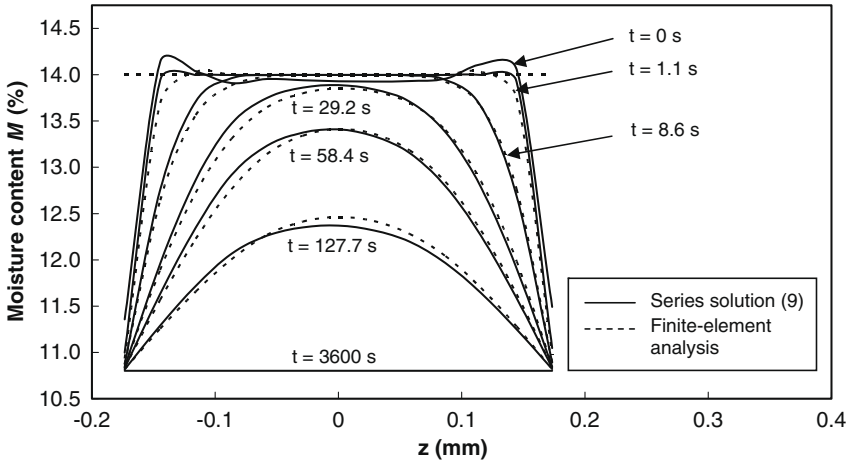

Fig. 2. Transient moisture content distribution for a three-layer paper sheet.

$$\varepsilon_x^0=\frac{\partial u^0}{\partial x}+\frac{1}{2}\left(\frac{\partial w^0}{\partial x}\right)^2 \quad \varepsilon_y^0=\frac{\partial v^0}{\partial y}+\frac{1}{2}\left(\frac{\partial w^0}{\partial y}\right)^2 \quad \gamma_{xy}^0=\frac{\partial u^0}{\partial y}+\frac{\partial v^0}{\partial x}+\frac{\partial w^0}{\partial x}\frac{\partial w^0}{\partial y}$$
$$\kappa_x=-\frac{\partial^2 w^0}{\partial x^2} \quad \kappa_y=-\frac{\partial^2 w^0}{\partial y^2} \quad \kappa_{xy}=-2\frac{\partial^2 w^0}{\partial x\partial y}, \tag{16}$$

where the u^0, v^0, and w^0 are the displacements of the midplane in the x-, y-, and z-directions. Note that in the above equation the geometric nonlinearities in the sense of von Karman are included. The displacement components are approximated using the following polynomials:

$$u^0(x,y)=cx-a^2\frac{x^3}{6}-abx\frac{y^2}{4} \tag{17a}$$
$$v^0(x,y)=dy-b^2\frac{y^3}{6}-aby\frac{x^2}{4} \tag{17b}$$
$$w^0(x,y)=\frac{1}{2}(ax^2+by^2) \tag{17c}$$

where the coordinates x and y are measured from the geometric center of the initially flat sheet. In these equations, parameters a and b represent the negative of the curvatures in the x- and y-directions, respectively. Parameters c and d represent the portion of the strains in the x-and y-directions that are

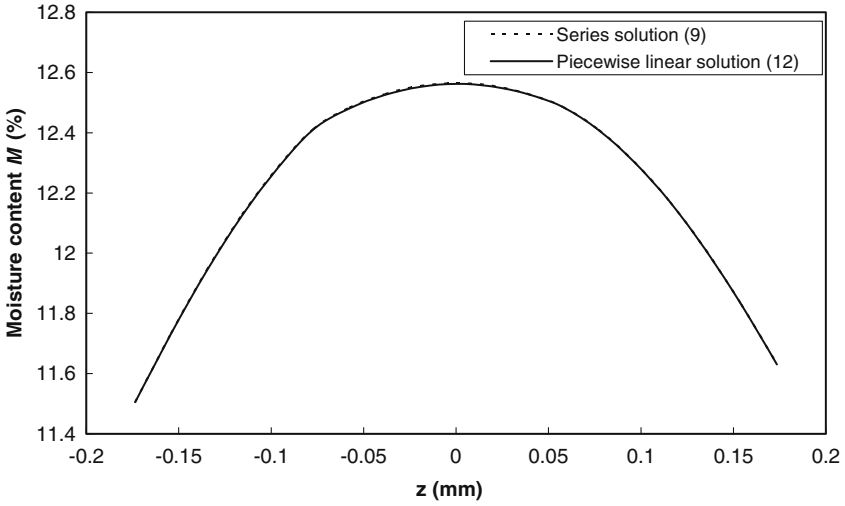

Fig. 3. Piecewise linear approximation of the moisture content distribution (t = 200 s).

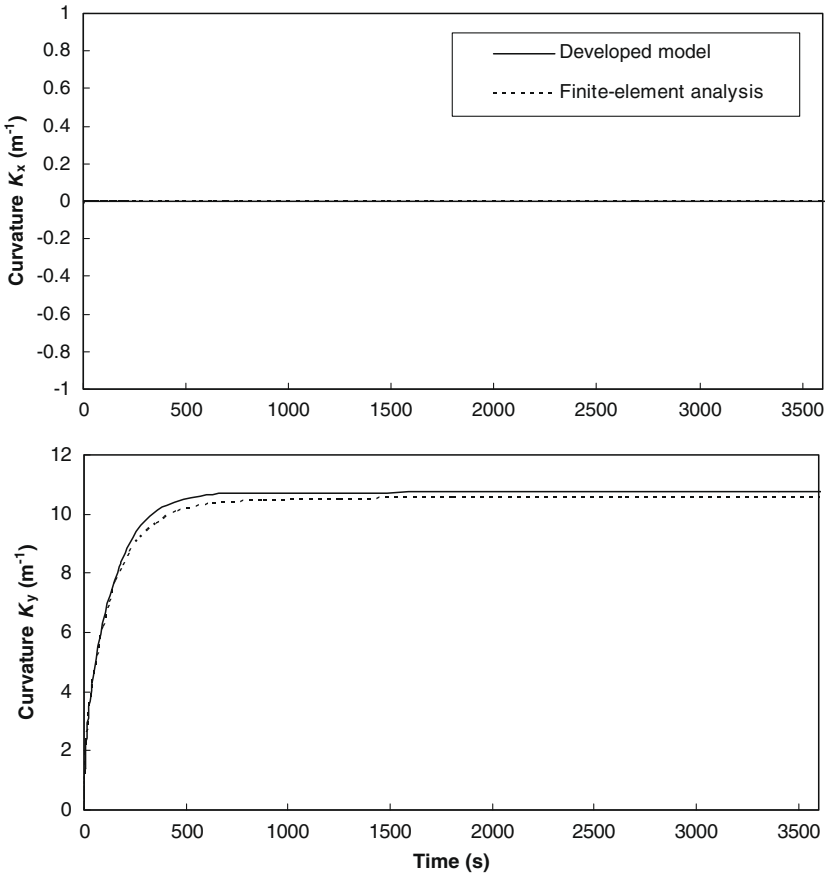

Fig. 4. Curvatures of paper sheet versus time ($L_x = L_y$ = 0.1 m).

constant. These four parameters completely define the shape of the sheet.

Back-substituting the assumed displacements into the definition of the midplane strains and curvatures, Eq. (16), and into the total potential energy expression, Eq. (13), the spatial integrations over x and y can be carried out. Finally, the moisture content change function, Eq. (14), can be substituted into Eq. (13) and the spatial integration over z can be calculated. The final result is an algebraic expression for the total potential energy of the form

$$\Pi = \Pi(a, b, c, d), \tag{18}$$

which is valid for a particular time $t = t_p$. Obviously, Π is also a function of the layer material and geometric properties and implicitly depends on the initial and boundary conditions used in the diffusion model.

2.2.2. Minimization of the total potential energy

To study the deformation of the sheet caused by the change in moisture content the variation of the total potential energy is used. This is done by allowing variations of the four displacement coefficients a, b, c, and d in Eq. (18),

$$\Pi(a + \delta a, b + \delta b, c + \delta c, d + \delta d) = \Pi(a, b, c, d) + \Delta\Pi, \tag{19}$$

where

$$\Delta\Pi = \delta\Pi + \frac{1}{2}\delta^2\Pi + \frac{1}{6}\delta^3\Pi + \frac{1}{24}\delta^4\Pi. \tag{20}$$

The quantities $\delta\Pi$, $\delta^2\Pi$, and $\delta^4\Pi$ are the first through fourth variations of Π, respectively. The first variation can be expressed as

$$\delta\Pi = f_a(a, b, c, d)\delta a + f_b(a, b, c, d)\delta b + f_c(a, b, c, d)\delta c + f_d(a, b, c, d)\delta d. \tag{21}$$

Equating the first variation to zero results in four nonlinear equilibrium equations of the form

$$\begin{aligned} f_a(a, b, c, d) &= 0 \\ f_b(a, b, c, d) &= 0 \\ f_c(a, b, c, d) &= 0 \\ f_d(a, b, c, d) &= 0. \end{aligned} \tag{22}$$

Solving these equations for a particular time $t = t_p$ gives the configuration of the sheet as it is subjected to a transient change in moisture content. The stability of the configuration is assessed by examining the second variation of the total potential energy. The overall procedure has been implemented using *MATHEMATICA*®.

2.3. Numerical results

In this section the developed model is used to study the response of a paper sheet subjected to transient moisture diffusion. The sheet has a square shape with a 0.1-m side-length ($L_x = L_y = 0.1$ m) and is composed of three layers. The properties of these layers are given in Table 1. All properties were determined experimentally (Bourque, 2008). Since the layers have different properties, the sheet is unsymmetric relative to its midplane. Initially, the sheet is flat and has a uniform moisture content (M_0) of 14% which corresponds to ambient air at 75% relative humidity (RH_0). Suddenly, a 10.8%-moisture content (M_∞) is applied to the outer surfaces which corresponds to air at 50% relative humidity

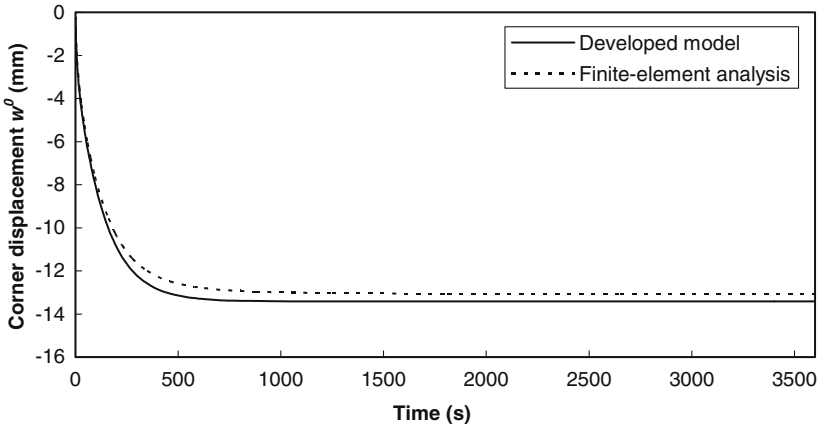

Fig. 5. Out-of-plane displacement of paper sheet corner versus time ($L_x = L_y = 0.1$ m).

Table 2
Properties of the NPB cardboard.

Layer	h (mm)	ρ (kg/m^3)	E_x (GPa)	E_y (GPa)	G_{xy} (GPa)	ν_{yx}	β_x (10^{-3}/%)	β_y (10^{-3}/%)	D (10^{-11} m^2/s)
1	0.059	1034	7.1	1.3	2.19	0.16	0.14	1.72	5.7
2	0.405	548	1.8	0.6	0.98	0.09	0.30	1.34	5.7
3	0.042	857	7.5	1.7	1.58	0.15	0.28	1.94	5.7

Table 3
Properties of the PB cardboard.

Layer	h (mm)	ρ (kg/m^3)	E_x (GPa)	E_y (GPa)	G_{xy} (GPa)	ν_{yx}	β_x (10^{-3}/%)	β_y (10^{-3}/%)	D (10^{-11} m^2/s)
1	0.059	1373	5.9	1.5	2.36	0.17	0.16	1.30	5.7
2	0.405	578	1.9	0.8	1.17	0.11	0.32	1.04	5.7
3	0.042	833	4.2	1.4	1.46	0.16	0.34	1.92	5.7

(RH_∞). The values for the different moisture contents were determined from an equilibrium moisture-sorption isotherm (Bourque, 2008). The convective mass transfer coefficient at the two outer surfaces was evaluated at 5.39×10^{-6} kg/m^{2}s% using equations given in Siau (1995). During the moisture diffusion process the sheet develops curvature. The objective is to demonstrate the ability of the model to predict the moisture content distribution through the thickness of the sheet and the induced deformation as a function of time during the diffusion process. The predictions will be validated in the next section with finite-element analyses.

First, the developed model determines the distribution of the moisture content in the three-layer paper sheet as a function of time. Fig. 2 shows the through-thickness moisture content distribution predicted by Eq. (9) at different times. The dashed lines represented in the figure correspond to results from finite-element analyses and will be discussed later. At $t = 0$, moisture content is supposed to be constant and equal to 14%. Some deviations between the expected and approximate solution can be observed since a very large number of terms in the series solution is required to approximate a straight line. However, for larger times the predicted moisture content distribution is expected to be more accurate. As time increases, the moisture content in the sheet decreases. At $t = 3600$ s, steady state equilibrium is reached and the moisture content is constant and equal to 10.8%.

Next, at different particular times the moisture content distribution is approximated using the piecewise-linear function. An example of the results obtained using the piecewise-linear function is shown in Fig. 3. The figure represents the moisture content distribution in the three-layer paper sheet at $t = 200$ s. The dashed line corresponds to the series solution given by Eq. (9) whereas the full line represents the piecewise linear function defined by Eq. (12). The number of intervals used in the approximation is $J = 6$ (for each layer). As can be observed, the correlation between the moisture content distribution predicted by the series solution and the one predicted by the piecewise-linear function is excellent. The selected interval number seems to be sufficient and the value of $J = 6$ is kept for all subsequent analyses.

Finally, the deformation induced by the moisture content change predicted by the piecewise-linear function is computed. The results are presented in Figs. 4 and 5, in the form of curvatures in the x- and y-directions, i.e. ($-a$), ($-b$), and out-of-plane displacement w^0 at ($x = L_x/2$, $y = L_y/2$) versus time. The dashed lines repre-

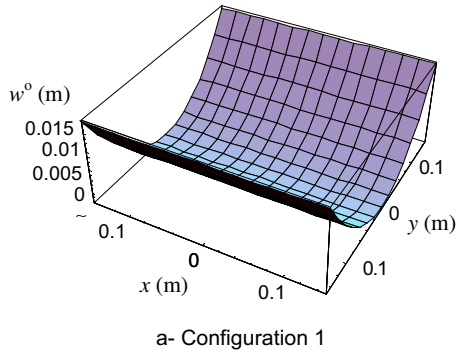

a- Configuration 1

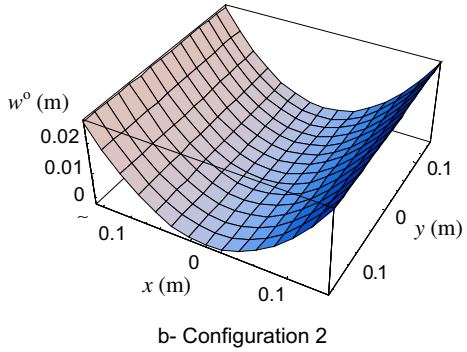

b- Configuration 2

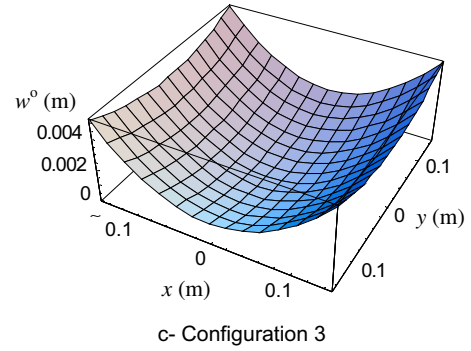

c- Configuration 3

Fig. 6. Equilibrium configurations predicted by the steady-state analysis for the NPB cardboard (obtained by Gendron et al. (2004)).

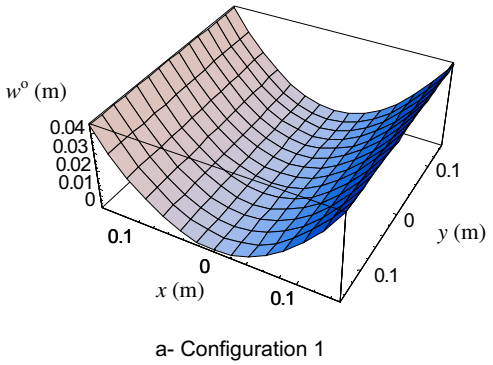

a- Configuration 1

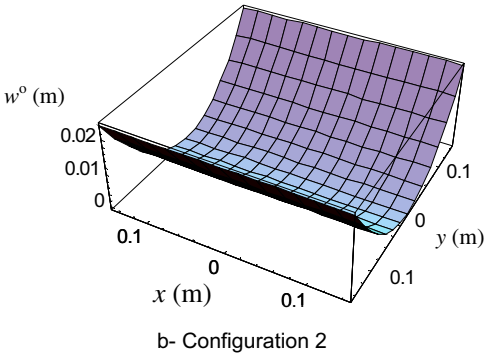

b- Configuration 2

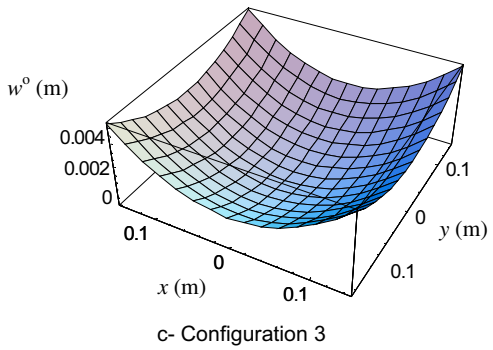

c- Configuration 3

Fig. 7. Equilibrium configurations predicted by the steady-state analysis for the PB cardboard (obtained by Gendron et al. (2004)).

sented in the figures correspond to results from finite-element analyses and will be discussed later. Referring to the figures, at $t = 0$, the curvatures and the corner displacement are zero since the sheet is initially flat. As soon as the moisture diffusion starts, the curvature in the y-direction and the corner displacement suddenly increases. The curvature in the x-direction remains zero through the diffusion process. Therefore, the sheet takes a cylindrical shape with its generator parallel to the x-axis. As time increases, the curvature and displacement keep increasing but at a slower rate. They attained constant values when steady state equilibrium is reached at $t = 3600$ s.

3. Finite-element analysis

To validate the numerical results obtained with the developed model, finite-element analyses were performed using the commercial software ABAQUS. The three-layer sheet was modelled using a mesh of 100 8-node-shell elements (S8RT). The sheet was free on the edges but clamped at the node at the geometric center of the sheet. Initial moisture content was applied and convective boundary conditions were specified at the outer surfaces. Geometric nonlinearities were taken into account and a fully transient coupled moisture-displacement analysis was performed. At each time increment, the moisture content distribution through the thickness was computed and the associated induced displacements obtained. Average values for the curvatures were obtained by fitting the out-of-plane displacement computed by ABAQUS with Eq. (17c). The moisture content distribution predicted by the finite-element analysis is represented in Fig. 2 for different times. As can be observed in the figure, the moisture content distributions computed by the present model correlate well with the finite-element predictions once the first second is passed. For $0 < t < 1$ s, the number of terms used in the series solution is not large enough to accurately predict the moisture content near the outer surfaces of the sheet. However, the present model quite accurately predicts the moisture content in the sheet away from the outer surfaces. The average curvatures determined from the finite-element analysis are presented as a function of time in Fig. 4. As predicted by the present model, the curvature in the x-direction remains zero. Correlation for the curvature in the y-direction is also very good. The curvature determined by the finite-element analysis is just slightly lower than the one predicted by the present model. Finally, the out-of-plane displacement predicted by the finite-element analysis at one of the sheet corners located at ($x = L_x/2$, $y = L_y/2$) is presented in Fig. 5. Good correlation can be observed at the beginning of the moisture diffusion process but as steady-state equilibrium is reached, the out-of-plane displacement predicted by the finite-element model is about 2% lower than the one predicted by the present model. From comparisons established between the finite-element analysis results and the predictions from the present model, it is clear that the model can

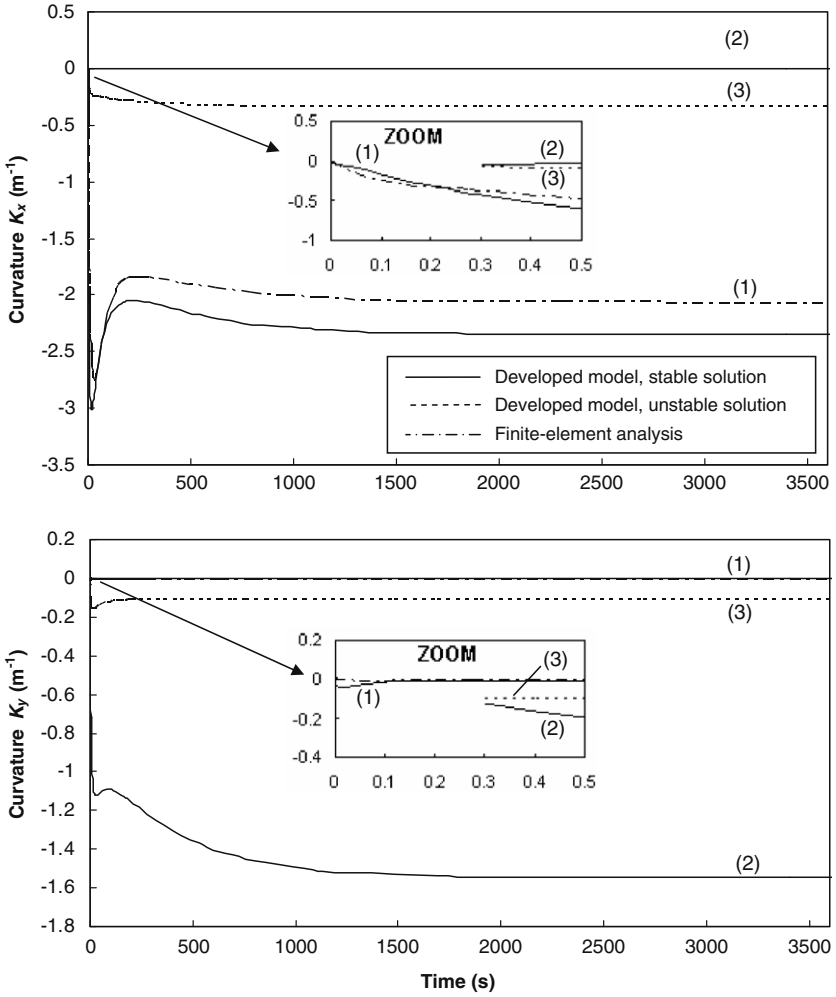

Fig. 8. Curvatures versus time for the NPB cardboard.

quite accurately predict the deformation induced by a transient change of moisture content in a multi-layer sheet. In the next section, the developed model is used to check the results of a study conducted by Gendron et al. (2004) on the hygro-mechanical deformation of two cardboard layups.

4. Case study

4.1. Steady-state response of the two cardboard layups

Gendron et al. (2004) studied the steady-state response of two cardboard layups subjected to a uniform change in moisture content. Each sheet had a three-layer unsymmetric construction. The properties of the two cardboard layers are given in Tables 2 and 3. The properties were determined experimentally except for the effective diffusion coefficient D which was assumed (Siau, 1995). One layup is designated PB and the other one NPB. The cardboard pieces were square with a 0.3-m side-length. The steady-state deformations induced by a 5%-moisture content change were predicted using a finite-element model and a semi-analytical model based on Hyer's (1981b) theory. Both models took non linear von Karman strain-displacement relationships into account. The finite-element model predicted that the final configuration of the NPB layup was cylindrical with a generator parallel to the x-axis. The maximum value for the out-of-plane displacement was 17.5 mm. For the PB layup, the final configuration predicted by the finite-element model was also cylindrical but with a generator parallel to the y-axis. The maximum value for the out-of-plane displacement was in this case 42.6 mm. The semi-analytical model predicted that both cardboard layups would have three steady-state equilibrium configurations as shown in Figs. 6 and 7. It was found that the two cylindrical shapes (1 and 2) are stable and that the bowl shape (3) is unstable. Among the two cylindrical shapes, configuration 1 presents the lowest energy and should be the actual equilibrium shape. It corresponds to the shape predicted by the finite-element analyses.

4.2. Transient response of the two cardboard layups

The model presented in this paper was used to predict the transient behaviour of the two cardboard layups subjected to a 5%-moisture content change. Properties given in Tables 2 and 3 were used and the convective mass transfer coefficient was assumed to be equal to 3.2×10^{-4} kg/m^{2}s% at the two outer surfaces (Cloutier and Gendron, 2001). The objective of the analyses is to study the ability of the developed model to predict the occurrence of multiple equilibrium configurations as a function of time.

The results of the transient model are presented in Figs. 8 and 9. Finite-element results are also presented in the figures and will be discussed later. Fig. 8 shows the curvatures in the x- and y-directions as a function of time for the NPB cardboard. At $t = 0$, the curvatures are zero and the sheet is flat. For

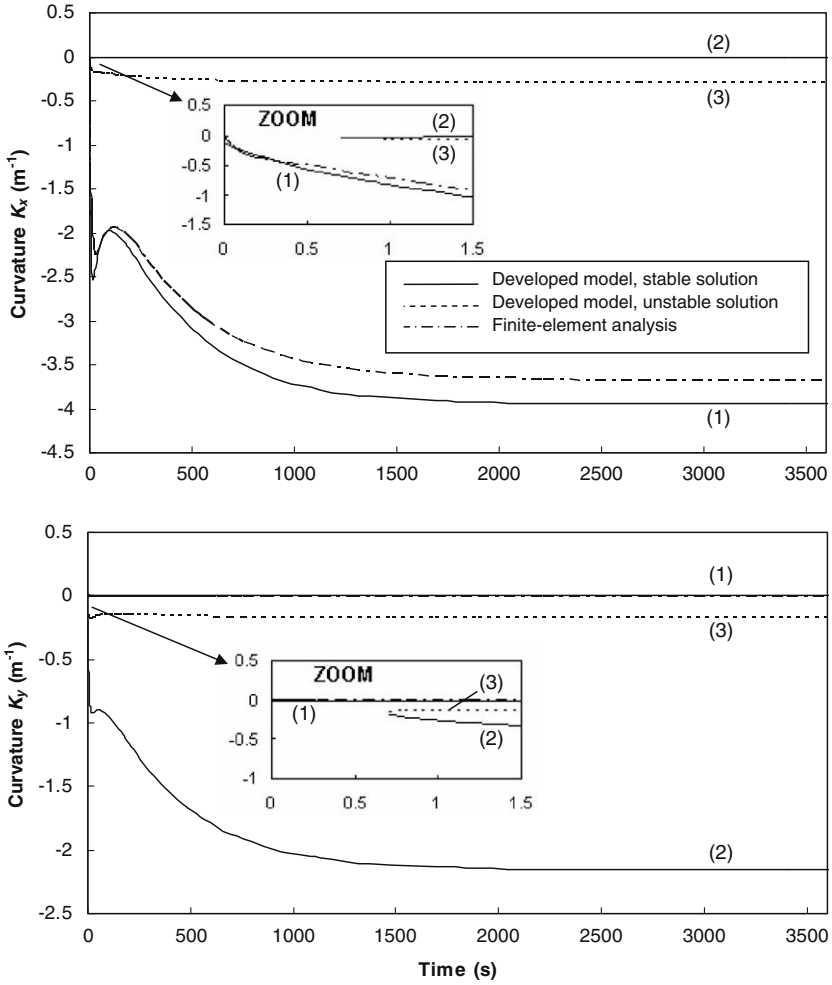

Fig. 9. Curvatures versus time for the PB cardboard.

$0 < t < 0.28$ s, curvature κ_x rapidly increases in magnitude whereas curvature κ_y first increases and then decreases to approach zero. There is only one solution, denoted (1) in the figure. From $t = 0.28$ s, two other solutions appear and remain present until steady-state equilibrium is reached. These solutions are denoted (2) and (3) in the graphs. When steady-state equilibrium is reached, solution (1) corresponds to a cylindrical shape with a generator parallel to the y-axis ($\kappa_x < 0$, $\kappa_y \cong 0$) whereas solution (2) corresponds to a cylindrical shape with a generator parallel to the x-axis ($\kappa_x \cong 0$, $\kappa_y < 0$). Solution (3) corresponds to a shallow bowl shape ($\kappa_x < 0$, $\kappa_y < 0$). A stability analysis shows that the bowl shape (3) is unstable and that the two cylindrical shapes (1) and (2) are stable. Shape (1) presents the lowest potential energy and should correspond to the actual equilibrium state.

Fig. 9 presents the curvatures in the x- and y-directions as a function of time predicted by the transient model for the PB cardboard. At $t = 0$, the curvatures are zero and the sheet is flat. For $0 < t < 0.7$ s, curvature κ_x rapidly increases in magnitude whereas curvature κ_y remains close to zero. There is only one solution, denoted (1) in the figure. From $t = 0.7$ s, two other solutions appear and remain present until the steady-state equilibrium is reached. These solutions are denoted (2) and (3) in the graphs. When steady-state equilibrium is reached, solution (1) corresponds to a cylindrical shape with a generator parallel to the y-axis ($\kappa_x < 0$, $\kappa_y \cong 0$). Solution (2) also corresponds to a cylindrical shape but with a generator parallel to the x-axis ($\kappa_x \cong 0$, $\kappa_y < 0$). Finally, solution (3) corresponds to a shallow bowl shape ($\kappa_x < 0$, $\kappa_y < 0$). A stability analysis shows that the bowl shape (3) is unstable and that the two cylindrical shapes (1) and (2) are stable. As for the NPB cardboard, shape (1) presents the lowest potential energy and should correspond to the actual equilibrium state.

Additionally, transient finite-element analyses were performed to validate the predictions obtained with the developed model for the two cardboards. The average curvatures determined from the finite-element analyses are presented as a function of time in Figs. 8 and 9. As is observed in the figures, the finite-element predictions follow solution (1) obtained with the developed model quite closely. The major curvature is just slightly lower than the one predicted by the developed model. The major curvatures for the NPB and the PB cardboards are, respectively, 11% and 6% lower than the ones predicted by the developed model. Finally, the out-of-plane displacement predicted for steady state condition by the finite-element analyses for the NPB and PB cardboards are presented in Figs. 10 and 11, respectively. For the purpose of comparison, the actual equilibrium shapes predicted by the developed model are indicated. As observed in the two figures, the shapes predicted by the finite-element analysis are identical to the ones predicted

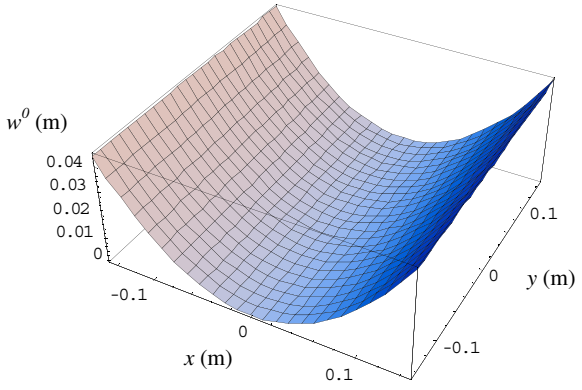

a- Configuration predicted by the transient developed model

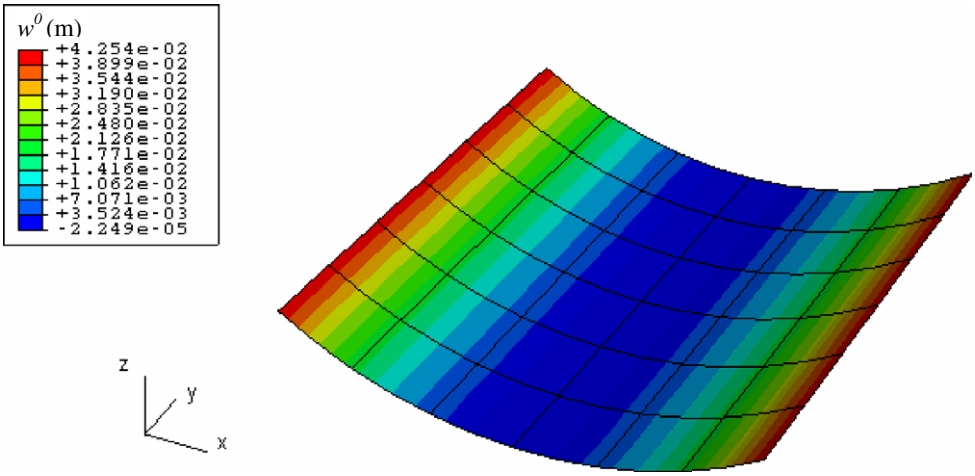

b- Configuration predicted by the transient finite-element analysis

Fig. 10. Actual equilibrium configurations predicted for the PB cardboard at $t = 3600$ s.

by the developed model. For the NPB cardboard, the maximum displacement predicted by the developed model is 26.4 mm which is very close to the value of 24.8 mm predicted by the finite-element analysis. For the PB cardboard, the maximum displacement predicted by the developed model is 44.4 mm compared to the value of 42.5 mm obtained with the finite-element model.

4.3. Discussion

The predictions obtained with the transient analyses can be compared to the ones obtained with the steady-state analyses by Gendron et al. (2004). First, considering the PB cardboard, the equilibrium shapes predicted by the transient analyses shown in Fig. 11 are similar to the one predicted by the steady-state analysis shown in Fig. 7a. However, for the NPB cardboard the shapes are not the same. The steady state analysis predicted that the shape was cylindrical with a generator parallel to the x-axis as shown in Fig. 6a. Curiously, the transient analyses predicted that the shape was cylindrical but with a generator parallel to the y-axis as shown in Fig. 10. The maximum displacement is also larger for the transient analysis than for the steady-state analysis (26.4 mm against 17.5 mm). Although surprising, this result is very interesting. It indicates that to adequately predict the hygro-mechanical deformation in a multi-layer paper or cardboard sheet the transient diffusion of moisture through the sheet thickness needs to be taken into account.

5. Summary and conclusions

This paper has presented the transient response of multi-layer sheets made of paper or cardboard subjected to moisture diffusion through the thickness. A model using de Monte's (2002) technique to solve the moisture diffusion equations and based on Hyer's (1981b) approach to predict the moisture-induced deformation has been developed. The model predicts the through-thickness moisture content distribution as a function of time. From these results, the moisture-induced deformation can be determined for different time values. The model was used to study the behaviour of a three-layer paper sheet and two three-layer cardboard sheets. Depending on the sheet type and the time values, the model predicts one or three equilibrium configurations. One of the three equilibrium configurations is always unstable. Among the two stable ones, the one which presents the lowest strain energy is considered as the actual equilibrium state. Finite-element analyses were also performed to validate the model predictions. Comparison between the predictions from the present model and the finite-element analyses demonstrate that the model can quite accurately predict the deformation behaviour of sheets subjected to transient moisture diffusion.

The predictions obtained for the two cardboard sheets were compared to predictions previously obtained using steady-state analyses. The comparison revealed important differences in the shapes predicted for one cardboard sheet. This result suggests that the moisture diffusion process may influence the configuration assumed by a sheet at steady-state equilibrium. Therefore, it is nec-

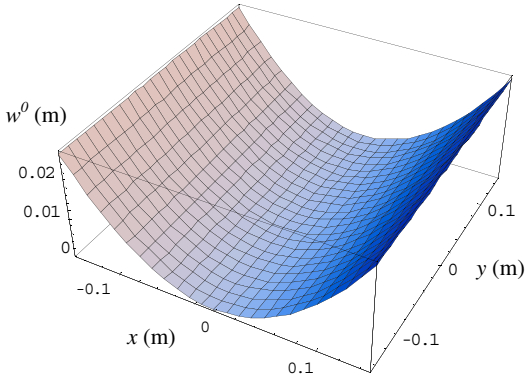

a- Configuration predicted by the transient developed model

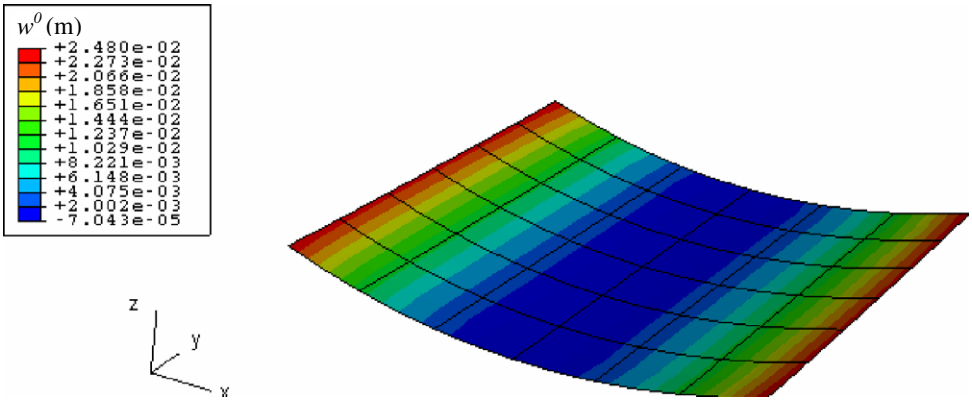

b- Configuration predicted by the transient finite-element analysis

Fig. 11. Actual equilibrium configuration for the NPB cardboard at $t = 3600$ s.

essary to take the moisture diffusion in the analysis into account to accurately predict the hygro-mechanical behaviour of paper or cardboard sheets.

Being able to predict the different equilibrium configurations as a function of time is important for studying and understanding the hygro-mechanical behaviour of paper or cardboard. It provides very valuable insight on whether a sheet may have a tendency to snap and change shape from one equilibrium configuration to another as relative humidity changes. The developed model also presents other advantages. It is simple to use, can perform computations quickly, and can be used for parametric studies.

Acknowledgement

This project was supported by the "Fonds québécois de la recherche sur la nature et les technologies". Their support was greatly appreciated.

References

Bandyopadhyay, A., Ramarao, B.V., Ramaswamy, S., 2002. Transient moisture diffusion through paperboard materials. Colloids and Surfaces A: Physicochemical and Engineering Aspects 206, 455–467.

Baronas, R., Ivanauska, F., 2004. Reducing spatial dimensionality in a model of moisture diffusion in a solid material. International Journal of Heat and Mass Transfer 47 (4), 699–705.

Bourque, J.-P., 2008. Etude des déformations hygromécaniques dans les feuilles de papier multicouches, M.S. Thesis, Department of Mechanical Engineering, Laval University, Québec, Canada.

Carlsson, L.A., 1981. Out-of-plane hygroinstability of multi-ply paperboard. Fiber Science and Technology 14, 201–212.

Chen, Y., Choong, E.T., Wetzel, D.M., 1995. Evaluation of diffusion coefficient and surface emission coefficient by an optimization technique. Wood and Fiber Science 27 (2), 178–182.

Cloutier, A., Gendron, G., 2001. Modélisation du gauchissement hygro-mécanique du carton. GIREF-RAP report May 9th 2001, Université Laval.

De Monte, F., 2002. An analytic approach to the unsteady heat conduction processes in one-dimensional composite media. International Journal of Heat and Mass Transfer 45 (6), 1333–1343.

Gendron, G., Dano, M.-L., Cloutier, A., 2004. A numerical study of the hygro-mechanical deformation of two cardboard layups. Composites Science and Technology 64 (5), 619–627.

Hägglund, R., Westerlind, B., Gulliksson, M., Nordstrand, T., 1999. Diffusion of water in paper. AIChE Symposium Series 95 (322), 71–79.

Hyer, M.W., 1981a. Some observations on the cured shape of thin unsymmetric lamaintes. Journal of Composite Materials 15, 175–194.

Hyer, M.W., 1981b. Calculations of the room temperature shapes of unsymmetric laminates. Journal of Composite Materials 15, 296–310.

Lu, W., Carlsson, L.A., 2001. Influence of viscoelastic behaviour on curl of paper. Mechanics of Time-Dependent Materials 5 (1), 79–100.

Nordstrom, A., Gudmundson, P., Carlsson, L.A., 1998. Influence of sheet dimensions on curl of paper. Journal of Pulp and Paper Science 24 (1), 18–25.

Siau, J.F., 1995. Wood: influence of moisture on physical properties, Dept. of Wood Science and Forest Products, Virginia Polytechnic Institute and State University.

Skaar, C., 1958. Moisture movement in beech below the fiber saturation point. Forest Product Journal 8, 352–357.

Wolfram, S., 1996. The Mathematica Book, third ed. Wolfram Media/Cambridge University Press.